Nanomaterials

Lecture 14: Nanoelectronic Alternatives

Nanoelectronic Alternatives

Carbon Nanotube Transistors

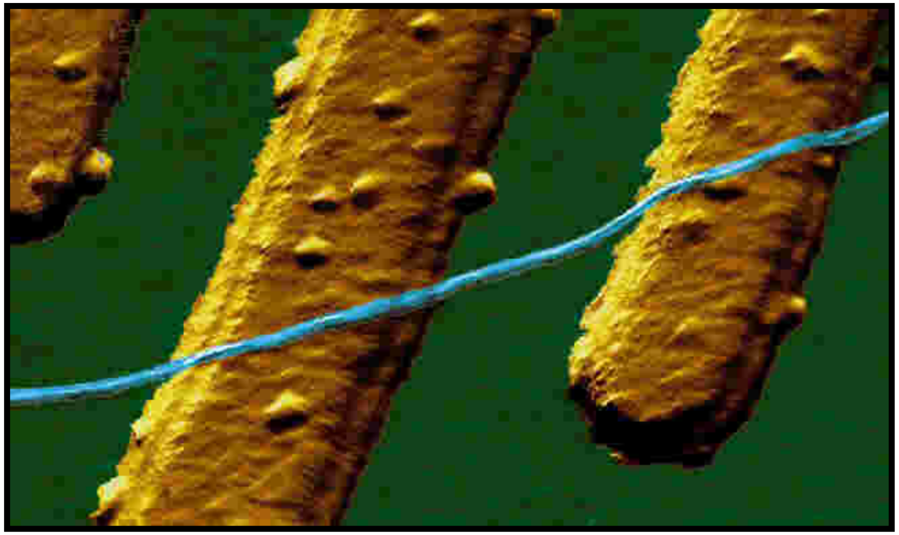

Nature, **391**, 59 (1998).

Molecular Electronics

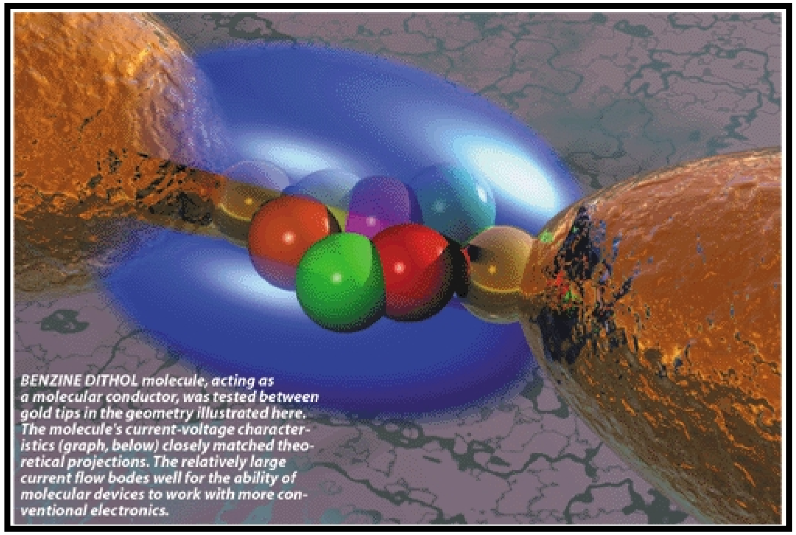

BENZINE DITHOL molecule, acting as a molecular conductor, was tested between gold tips in the geometry illustrated here. The molecule's current-voltage characteristics (graph, below) closely matched theoretical projections. The relatively large current flow bodes well for the ability of molecular devices to work with more conventional electronics.

Sci. American, **282**, 86 (2000).

Resonant Tunneling Diodes, Single Electron Devices, Quantum Cellular Automata, Molecular Electronics, …

Nanoelectronic Predictions

Projected timeline for the electronics industry:

A. C. Seabaugh, P. Mazumder,
***Proceedings of the IEEE*, 87, 535 (1999).**

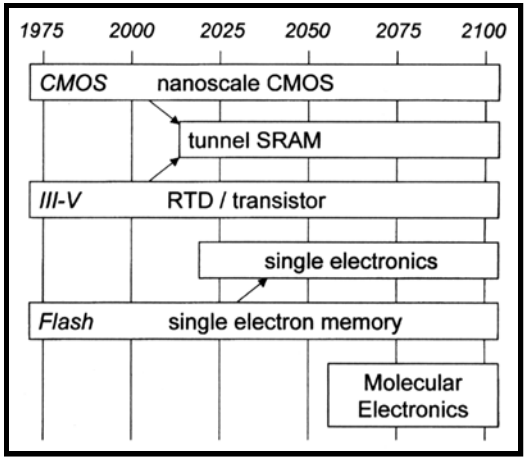

EXECUTIVE OFFICE OF THE PRESIDENT OF THE UNITED STATES

President William J. Clinton
State of the Union Address
January 27, 2000

"Soon researchers will bring us devices that can translate foreign languages as fast as you can talk; materials 10 times stronger than steel at a fraction of the weight; ***and -- this is unbelievable to me -- molecular computers the size of a tear drop with the power of today's fastest supercomputers.***"

Resonant Tunneling Diode

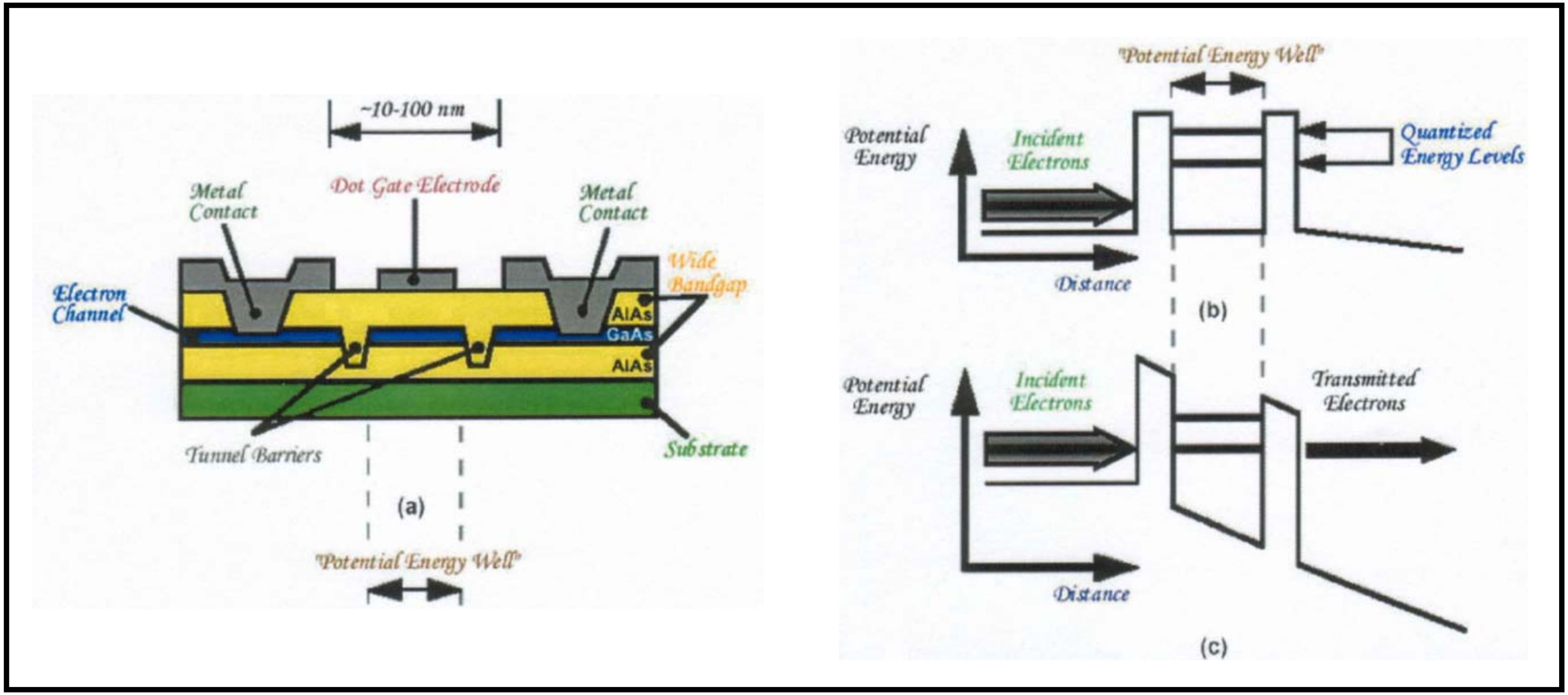

http://courses.nus.edu.sg/course/phyweets/Projects99/Quantum

Negative Differential Resistance

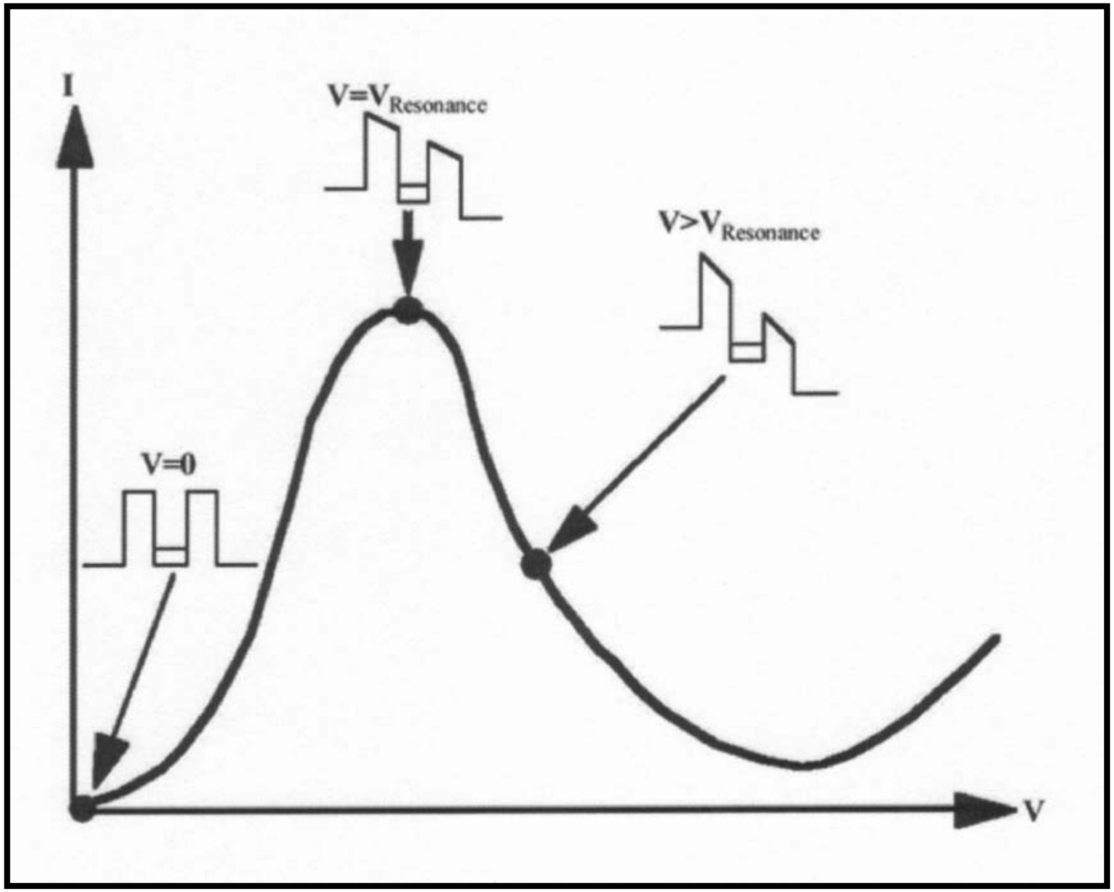

http://courses.nus.edu.sg/course/phyweets/Projects99/Quantum

Single Electron Devices

Coulomb Blockade: Suppression of electron tunneling to an island (0-D quantum dot) by a single electron charging energy

NOTE: Capacitor charging energy = $Q^2/2C$

For a single electron → $e^2/2C$

Two Conditions for Coulomb Blockade:

(1) Thermal Fluctuations: $e^2/C >> kT$

(2) Heisenberg Uncertainty: $\Delta E \Delta t >> h$

$(e^2/C)(R_tC) >> h \rightarrow R_t >> h/e^2$

Temperature Requirement for Coulomb Blockade

Temperature Condition for Coulomb Blockade:

To suppress thermal fluctuations, $e^2/C >> kT$

→ For room temperature operation, C ~ 1 aF = 10^{-18} F

→ For C ~ 1 aF, quantum dot dimensions ~ 1 nm

→ Since it is challenging to fabricate down to 1 nm, most single electron devices only operate at low temperature

GaAs/AlGaAs Single Electron Device

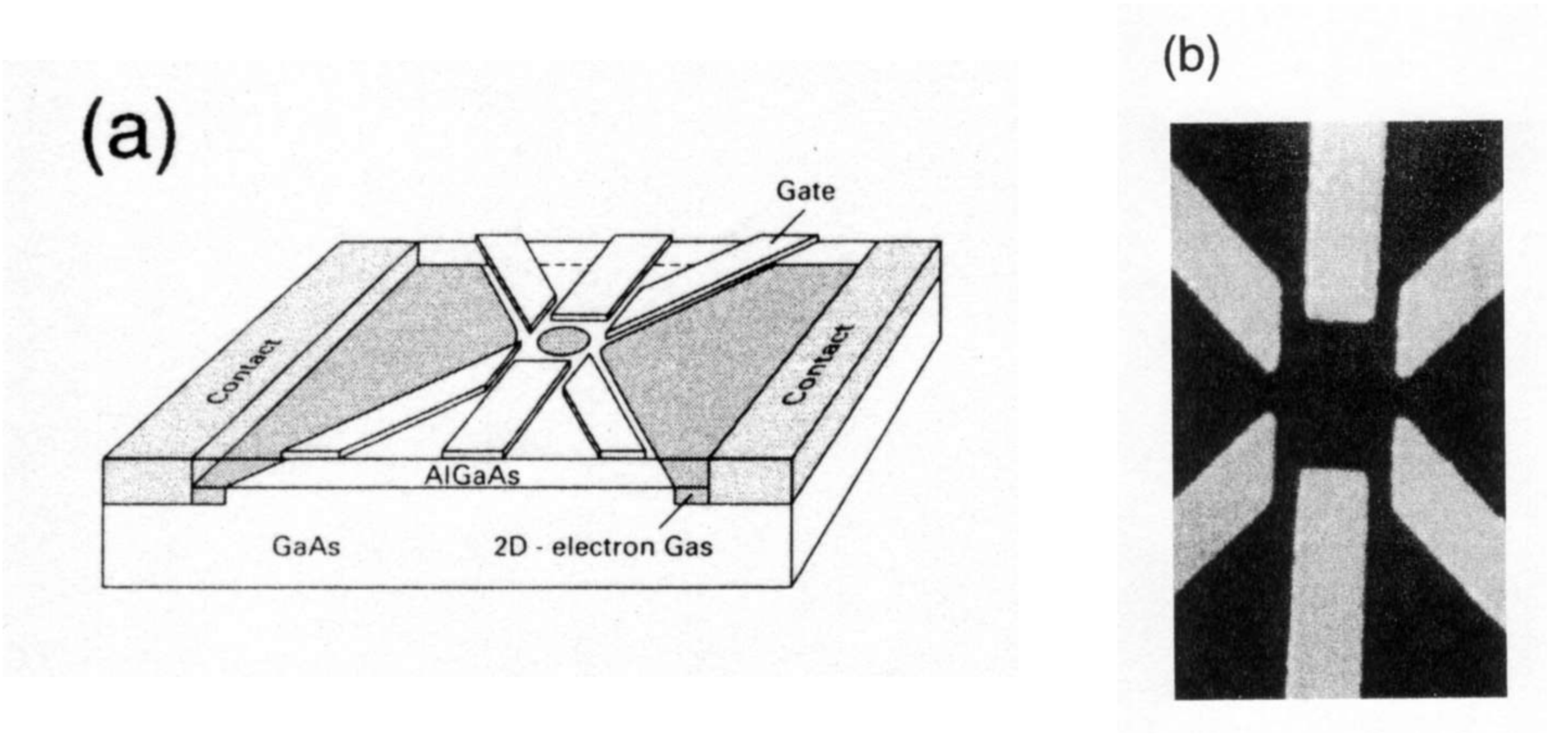

Top gates deplete 2-DEG, thus forming a quantum dot

Coulomb Blockade I-V Characteristic

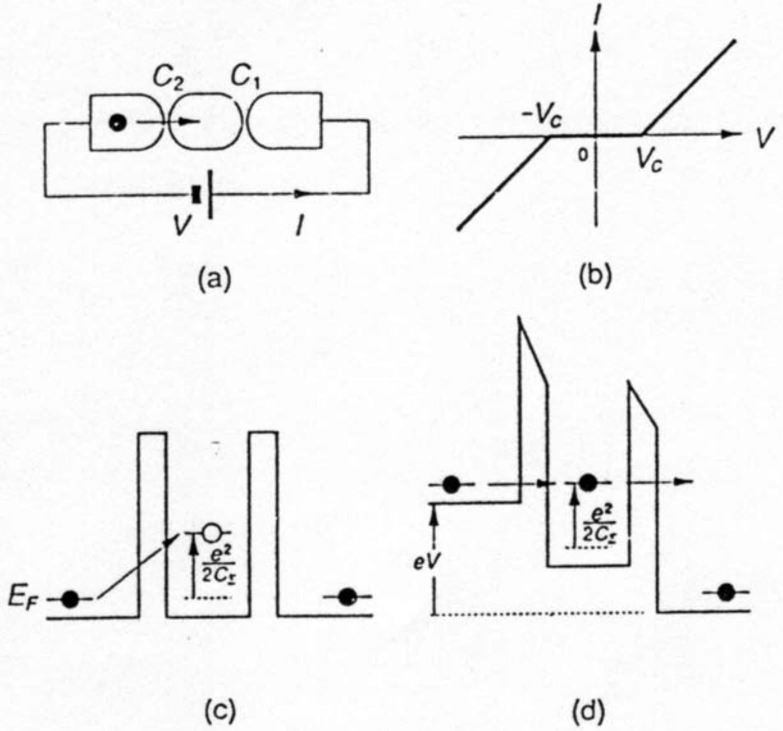

Fig. 1. (a) A one island system. (b) Coulomb blockade characteristic. (c) and (d) Energy barriers without and with applied bias. E_F is the electron fermi energy.

Single Electron Transistor

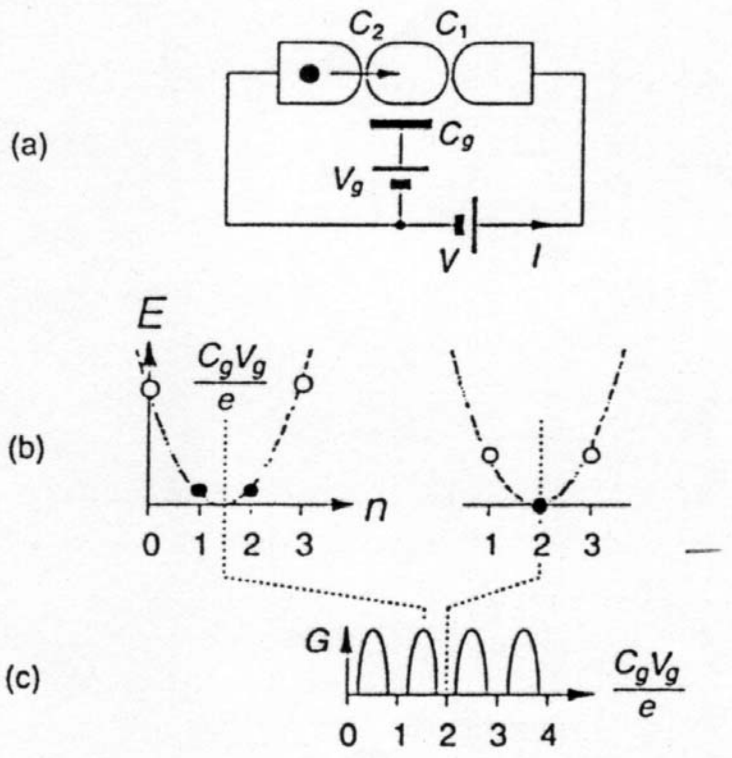

Fig. 2. Operating principle of a single electron transistor. (a) Configuration. (b) Charging energy as a function of the number of excess electrons on the central island. (c) Conductance as a function of gate voltage.

Single Electron Transistor

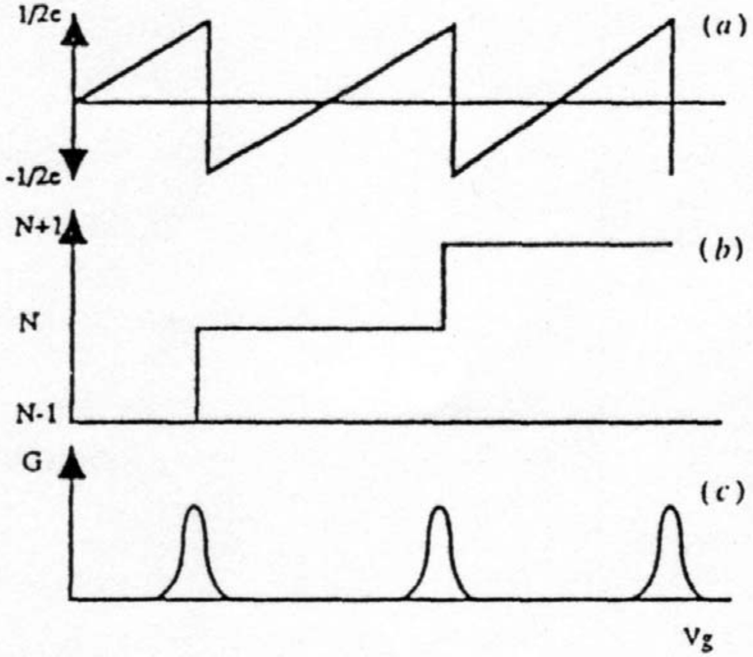

Fig. 3. A plot of: (a) charge; (b) number of electrons; and (c) conductance through a dot versus gate voltage.

Single Electronics

Benefits:

(1) Low power since only one electron moves through the device

(2) High device density is possible

Problems:

(1) Fabrication is difficult

(2) Inherently slow since only one electron moves through the device
→ Difficult to charge up capacitance at outputs (fan-out problems)

(3) Interconnections

Quantum Cellular Automata

Consider four coupled quantum dots:

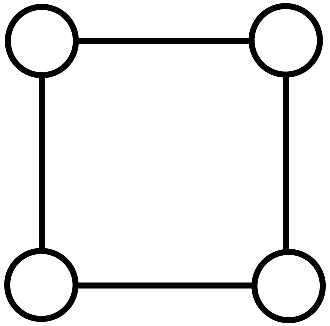

If two electrons are injected into this cell, there are two possibilities that minimize electrostatic energy:

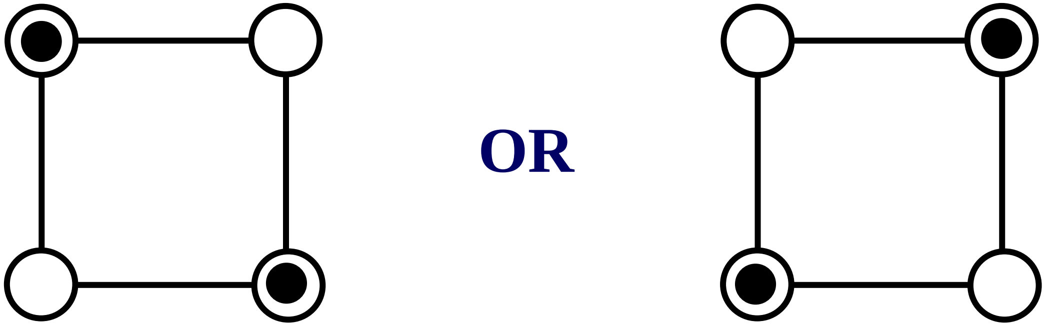

OR

“0” **“1”**

Quantum Cellular Automata

Adjacent QCA cells align to minimize electrostatic energy:

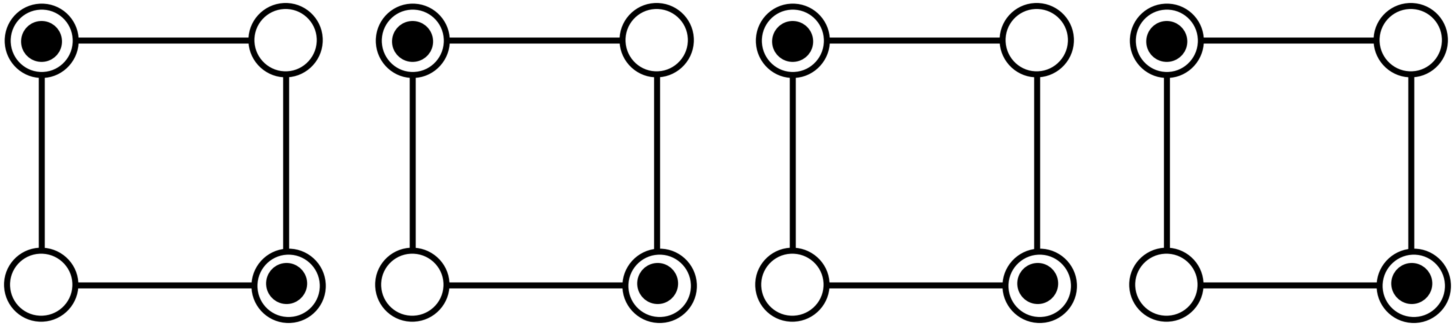

- If you switch the first cell, the other cells will follow

→ Information transfer without electron transfer
→ No interconnections are required between cells

- Intersecting QCA rows allow for logic and computation

Quantum Cellular Automata

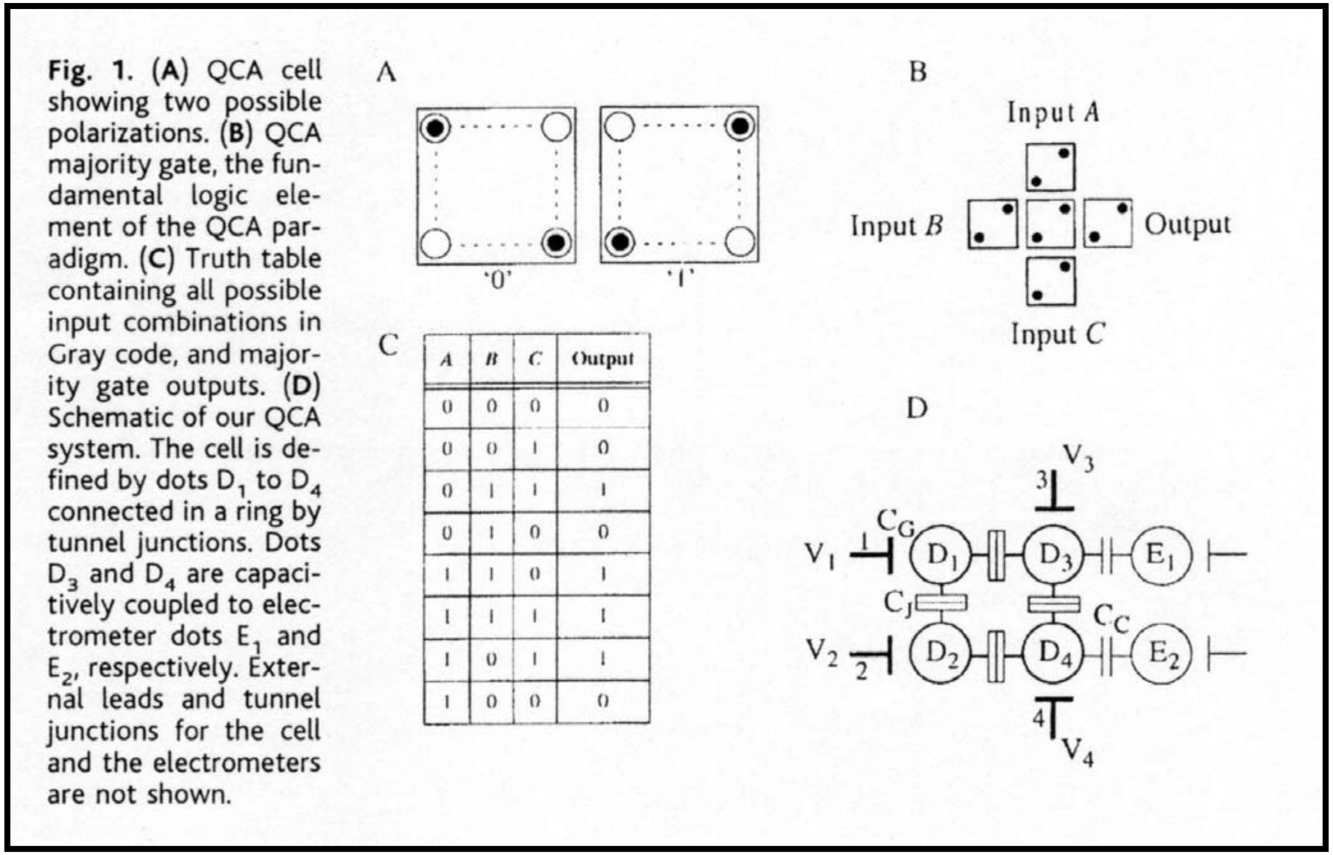

Fig. 1. (**A**) QCA cell showing two possible polarizations. (**B**) QCA majority gate, the fundamental logic element of the QCA paradigm. (**C**) Truth table containing all possible input combinations in Gray code, and majority gate outputs. (**D**) Schematic of our QCA system. The cell is defined by dots D_1 to D_4 connected in a ring by tunnel junctions. Dots D_3 and D_4 are capacitively coupled to electrometer dots E_1 and E_2, respectively. External leads and tunnel junctions for the cell and the electrometers are not shown.

A	*B*	*C*	Output
0	0	0	0
0	0	1	0
0	1	1	1
0	1	0	0
1	1	0	1
1	1	1	1
1	0	1	1
1	0	0	0

I. Amlani, *et al.*, *Science*, **284**, 289 (1999).

Quantum Cellular Automata

- Although QCA minimizes the number of interconnections, it still suffers from the same thermal fluctuation problems as single electronic devices
- Consequently, QCA must be implemented at low temperatures or at molecular length scales:

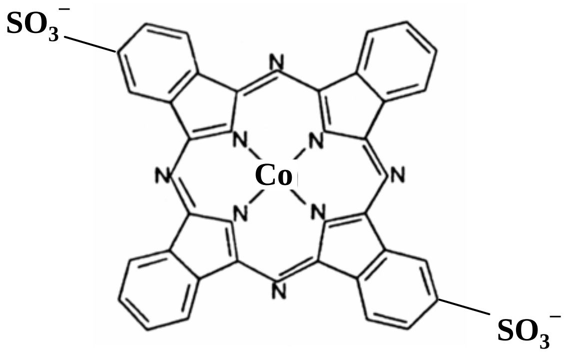

QCA Molecule

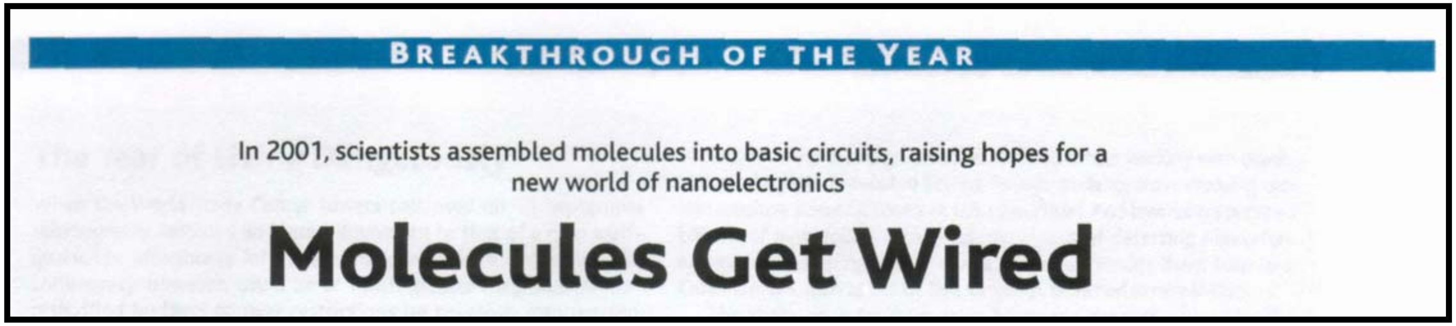

BREAKTHROUGH OF THE YEAR

In 2001, scientists assembled molecules into basic circuits, raising hopes for a new world of nanoelectronics

Molecules Get Wired

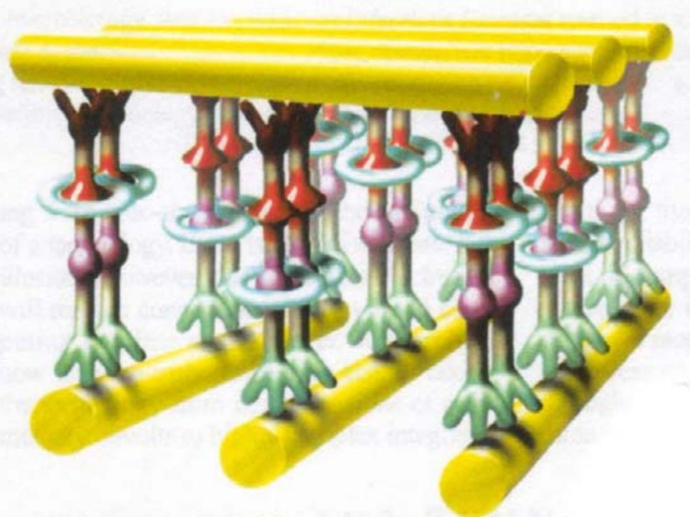

Good connections. Molecules can now be crafted into working circuits. Constructing real molecular chips will be a big challenge.

Science, **294**, 2442 (2001).

Contacting Molecules with Break Junctions

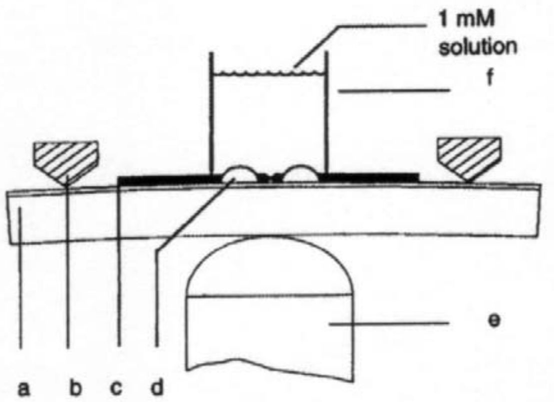

Fig. 1. A schematic of the MCB junction with (a) the bending beam, (b) the counter supports, (c) the notched gold wire, (d) the glue contacts, (e) the pizeo element, and (f) the glass tube containing the solution.

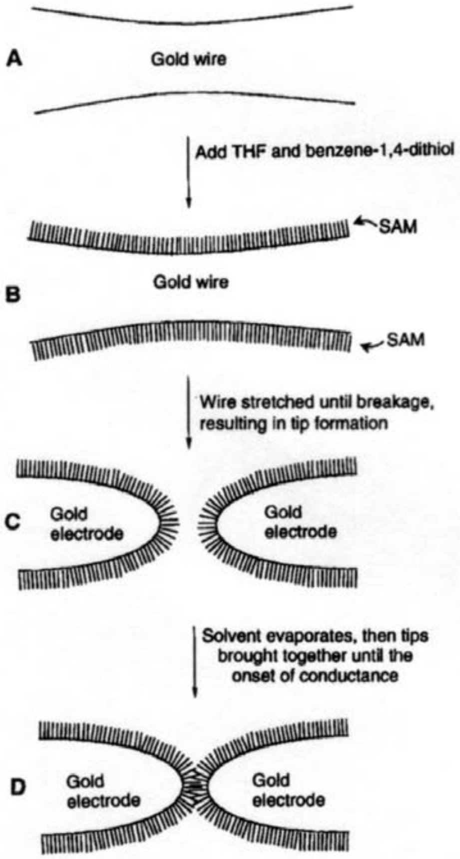

Fig. 2. Schematic of the measurement process. (**A**) The gold wire of the break junction before breaking and tip formation. (**B**) After addition of benzene-1,4-dithiol, SAMs form on the gold wire surfaces. (**C**) Mechanical breakage of the wire in solution produces two opposing gold contacts that are SAM-covered. (**D**) After the solvent is evaporated, the gold contacts are slowly moved together until the onset of conductance is achieved. Steps (C) and (D) (without solution) can be repeated numerous times to test for reproducibility.

M. A. Reed, *et al.*, *Science*, **278**, 252 (1997).

Room Temperature Molecular Conduction

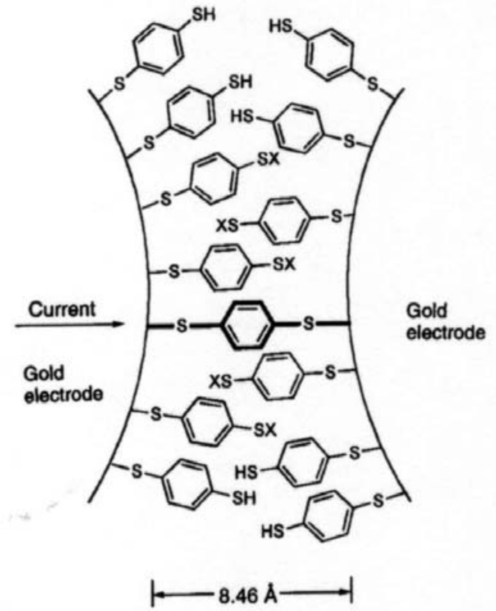

Fig. 3. A schematic of a benzene-1,4-dithiolate SAM between proximal gold electrodes formed in an MCB. The thiolate is normally H-terminated after deposition; end groups denoted as X can be either H or Au, with the Au potentially arising from a previous contact/retraction event. These molecules remain nearly perpendicular to the Au surface, making other molecular orientations unlikely (*21*).

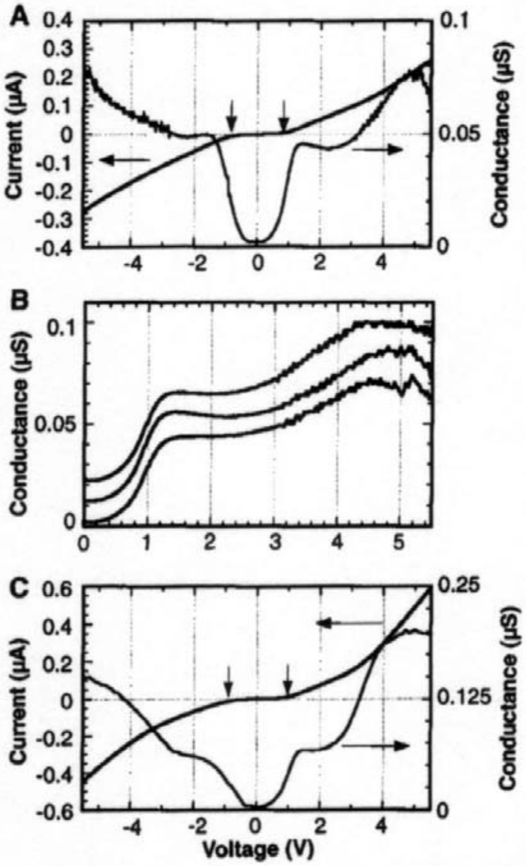

Fig. 4. (**A**) Typical *I*(*V*) characteristics, which illustrate a gap of 0.7 V; and the first derivative *G*(*V*), which shows a steplike structure. (**B**) Three independent *G*(*V*) measurements, offset for clarity, illustrating the reproducibility of the conductance values. The measurements were made with the same MCB but for different retractions/contacts and thus different contact configurations. Offsets of 0.01 μS for the middle curve and 0.02 μS for the top curve are used for clarity. The first step for these three measurements gives values of 22.2, 22.2, and 22.7 megohm (top to bottom); the next step gives values of 12.5, 13.3, and 14.3 megohm. The middle curve is the same data as in (A). (**C**) An *I*(*V*) and *G*(*V*) measurement illustrating conductance values approximately twice the observed minimum conductance values. Resistances of ~14 megohm for the first step and 7.1 megohm (negative bias) and 5 megohm (positive bias) for the second step were measured.

M. A. Reed, *et al.*, *Science*, **278**, 252 (1997).

Contacting Molecules with Nanoscale Pores

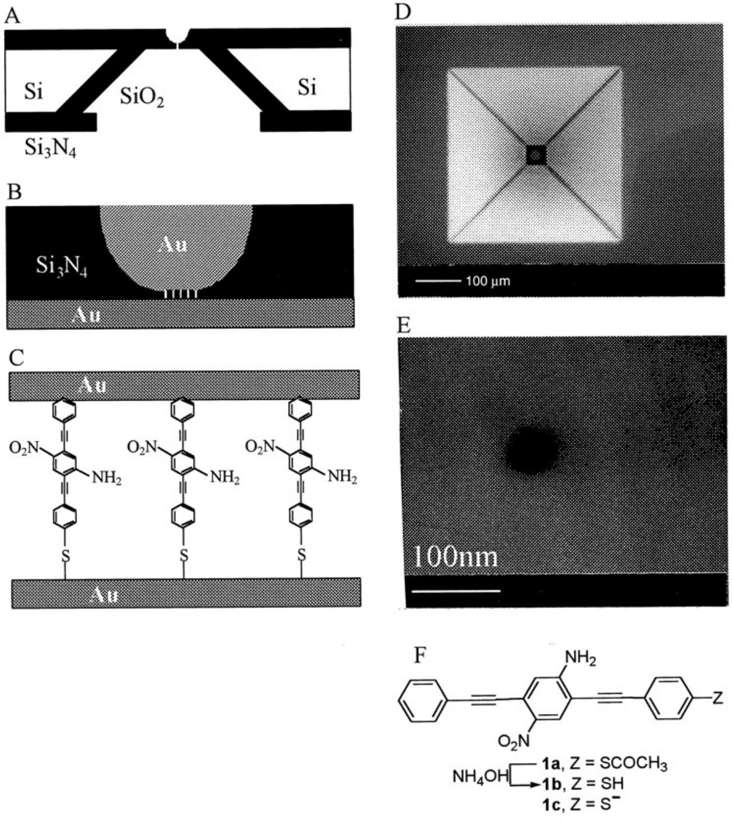

Fig. 1. Schematics of device fabrication. **(A)** Cross section of a silicon wafer with a nanopore etched through a suspended silicon nitride membrane. **(B)** Au-SAM-Au junction in the pore area. **(C)** Blowup of (B) with **1c** sandwiched in the junction. **(D)** Scanning electron micrograph (SEM) of pyramid Si structure after unisotropic Si etching [that is, *the bottom view of* (A)]. **(E)** SEM of an etched nanopore through the silicon nitride membrane. **(F)** The active molecular compound **1c** and its precursors the free thiol **1b** and the thiol-protected system **1a**.

J. Chen, *et al.*, *Science*, **286**, 1550 (1999).

Molecular Negative Differential Resistance

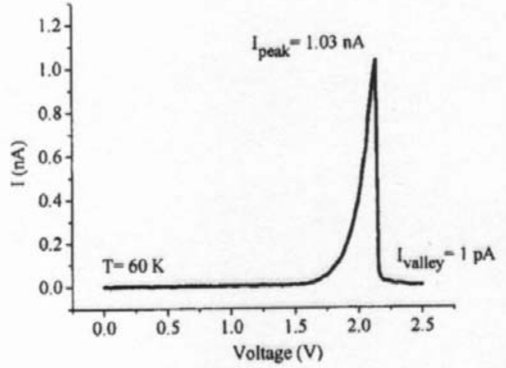

Fig. 2. $I(V)$ characteristics of a Au-(2′-amino-4-ethynylphenyl-4′-ethynylphenyl-5′-nitro-1-benzenethiolate)-Au device at 60 K. The peak current density is ~50 A/cm^2, the NDR is ~−400 μohm cm^2, and the PVR is 1030:1.

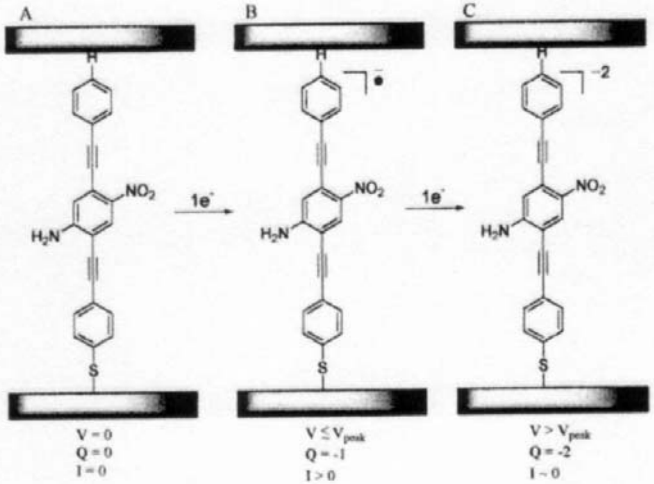

Fig. 4. Potential mechanism for the NDR effect. As voltage is applied, the molecules in the SAM (**A**) undergo a one-electron reduction to form the radical anion (**B**) that provides a conductive state. Further increase of the voltage causes another one-electron reduction to form the dianion insulating state (**C**). Q is the charge.

J. Chen, *et al.*, *Science*, **286**, 1550 (1999).

Recent Molecular Electronics Research

Metal-Molecule-Metal Junctions:

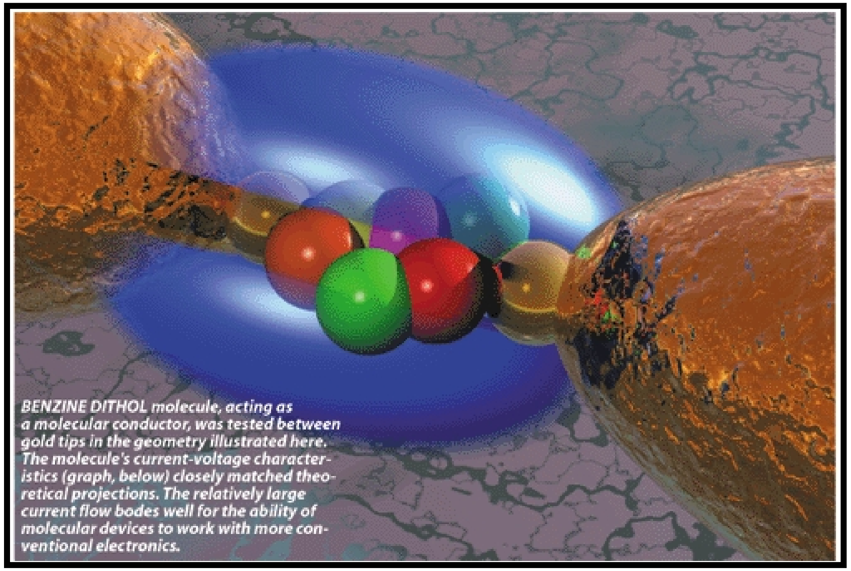

BENZINE DITHOL molecule, acting as a molecular conductor, was tested between gold tips in the geometry illustrated here. The molecule's current-voltage characteristics (graph, below) closely matched theoretical projections. The relatively large current flow bodes well for the ability of molecular devices to work with more conventional electronics.

Sci. American, **282**, 86 (2000).

Recent results suggest that the contacts play a large – if not dominant role – in molecular electronic devices.

Science, **300**, 1384 (2003).

Semiconductor-Molecule-Metal Junctions

Molecular Resonant Tunneling Diode (RTD):

Negative Differential Resistance (NDR)

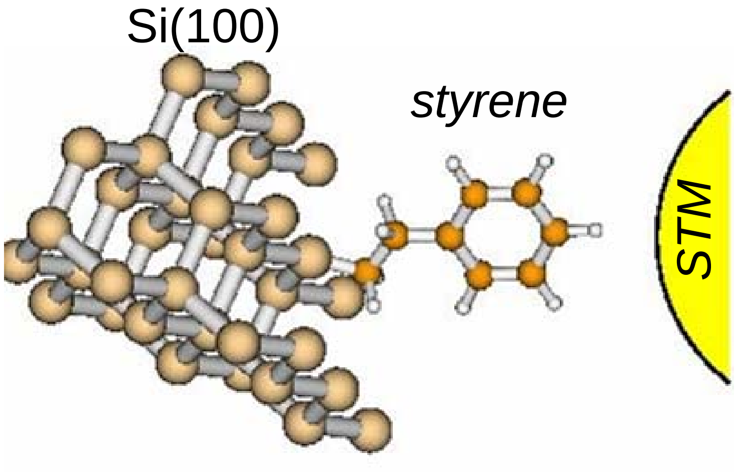

Tunneling probability versus energy:

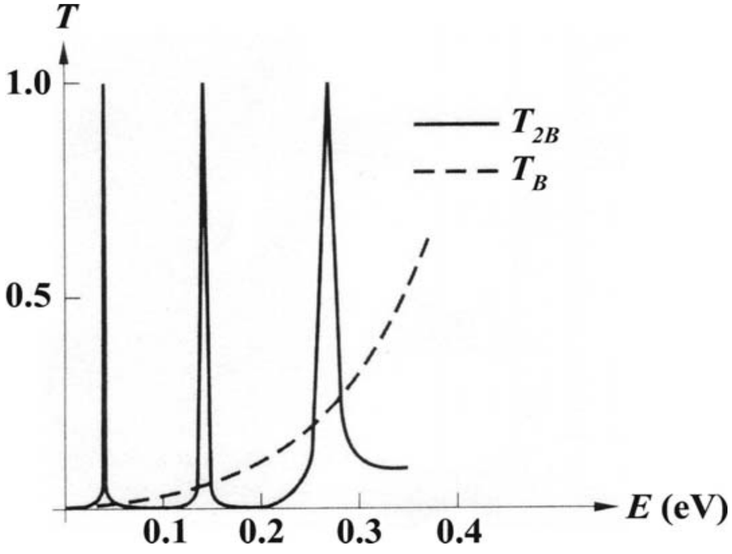

Calculated I-V Curve:

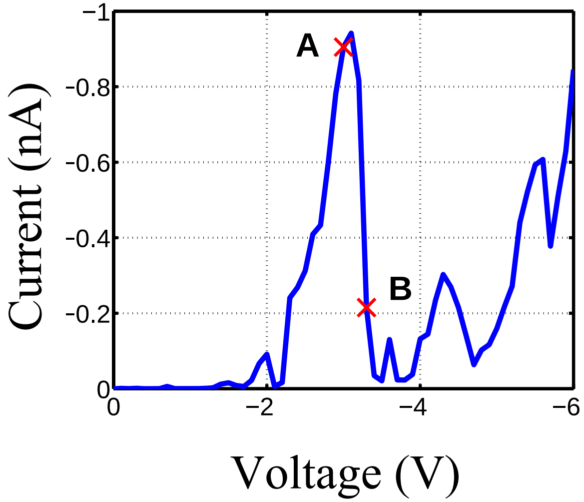

Experimental Approach

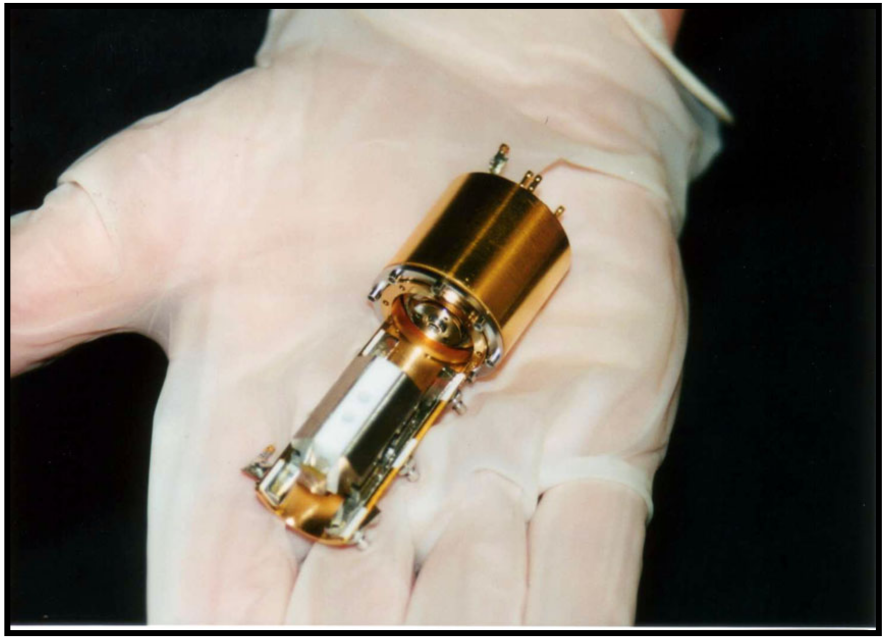

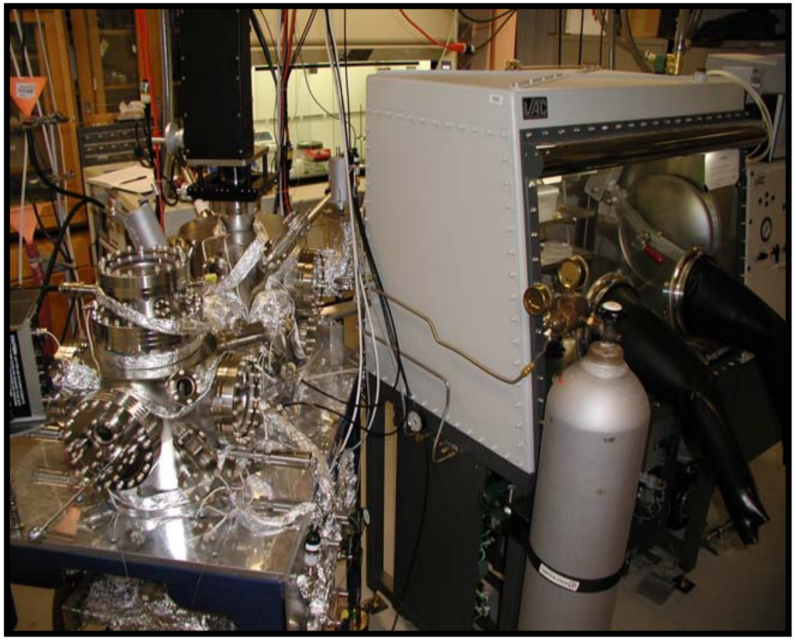

- **Fundamental scanning tunneling microscopy experiments in ultra-high vacuum at room temperature**
- **Studies on silicon bridge the gap between fundamental research and modern technology**

Styrene on the Si(100)-2×1 Surface

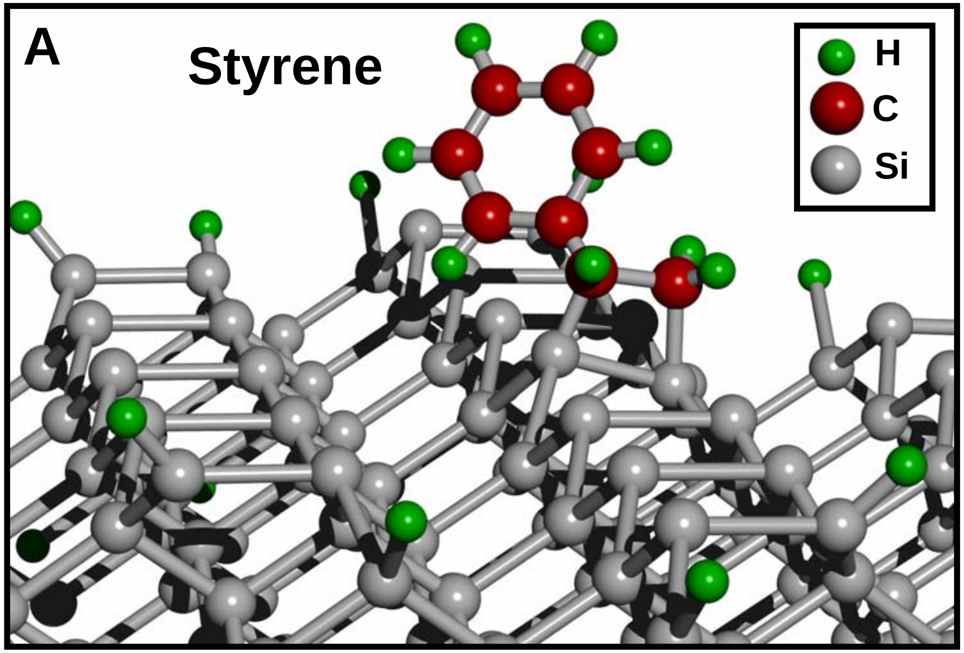

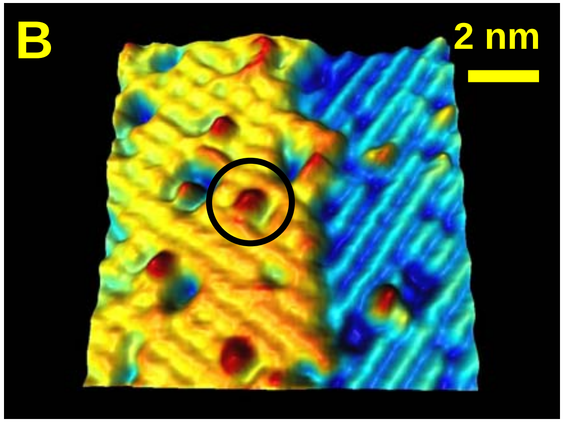

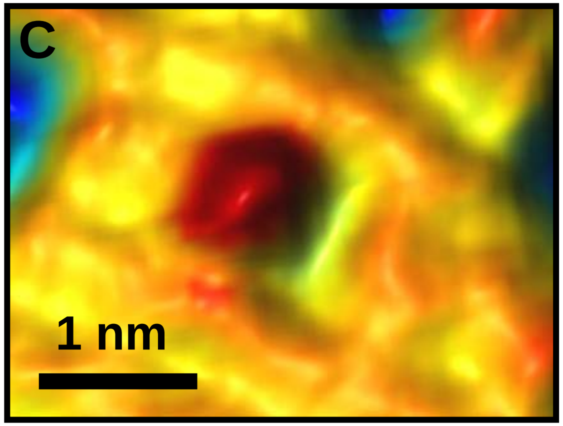

Individual styrene molecules are probed with the STM

N. P. Guisinger, *et al.*, *Nano Letters*, **4**, 55 (2004).

I-V Curve for Styrene on n^+-Si(100)

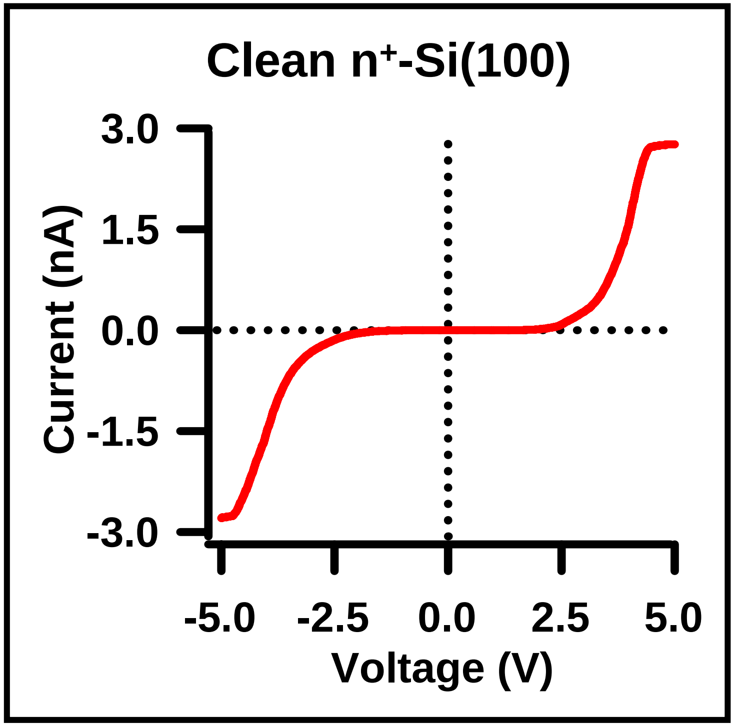

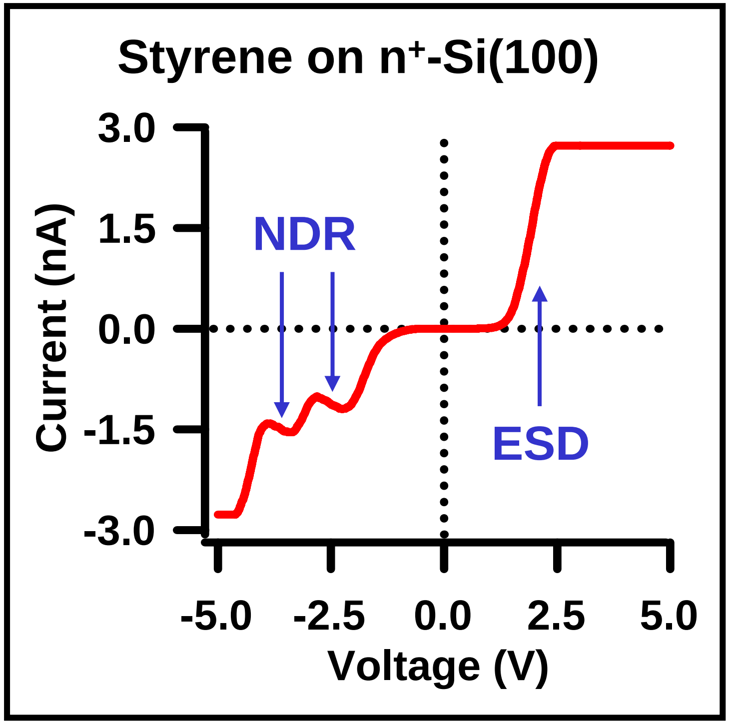

- Multiple NDR events.
- NDR is only observed at negative sample bias.
- Molecule is desorbed from the surface at positive bias.

TEMPO on the Si(100)-2×1 Surface

TEMPO:
(2,2,6,6-tetramethyl-1-piperidinyloxy)

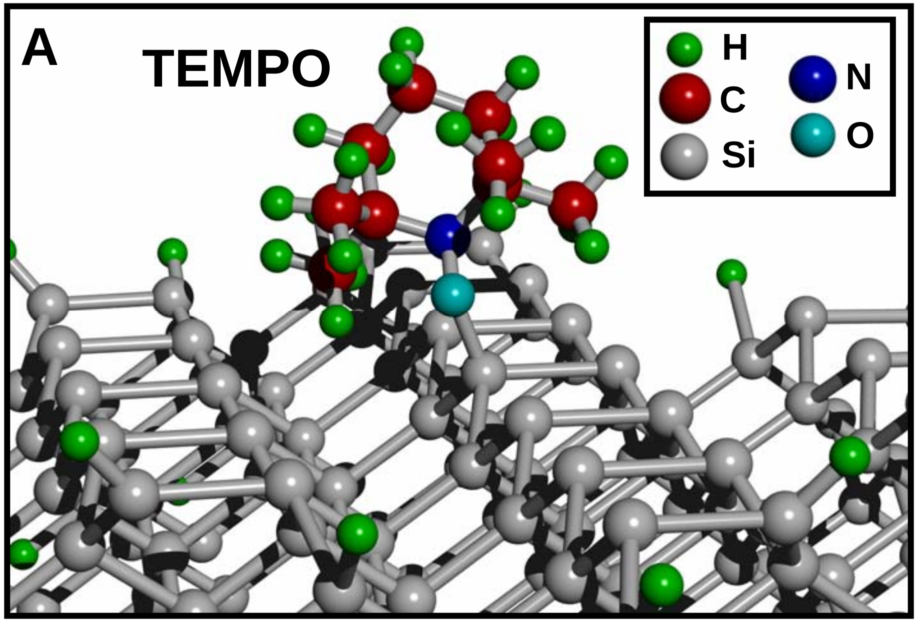

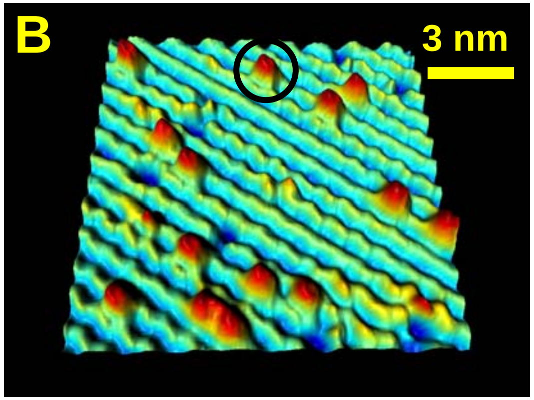

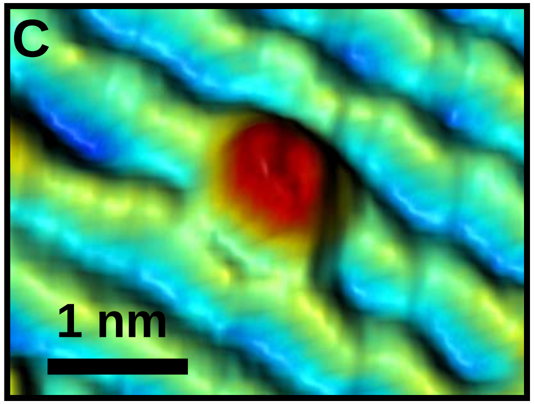

TEMPO resists electron stimulated desorption since it is a saturated hydrocarbon

N. P. Guisinger, *et al.*, *Nano Letters*, **4**, 55 (2004).

I-V Curve for TEMPO on n$^+$-Si(100)

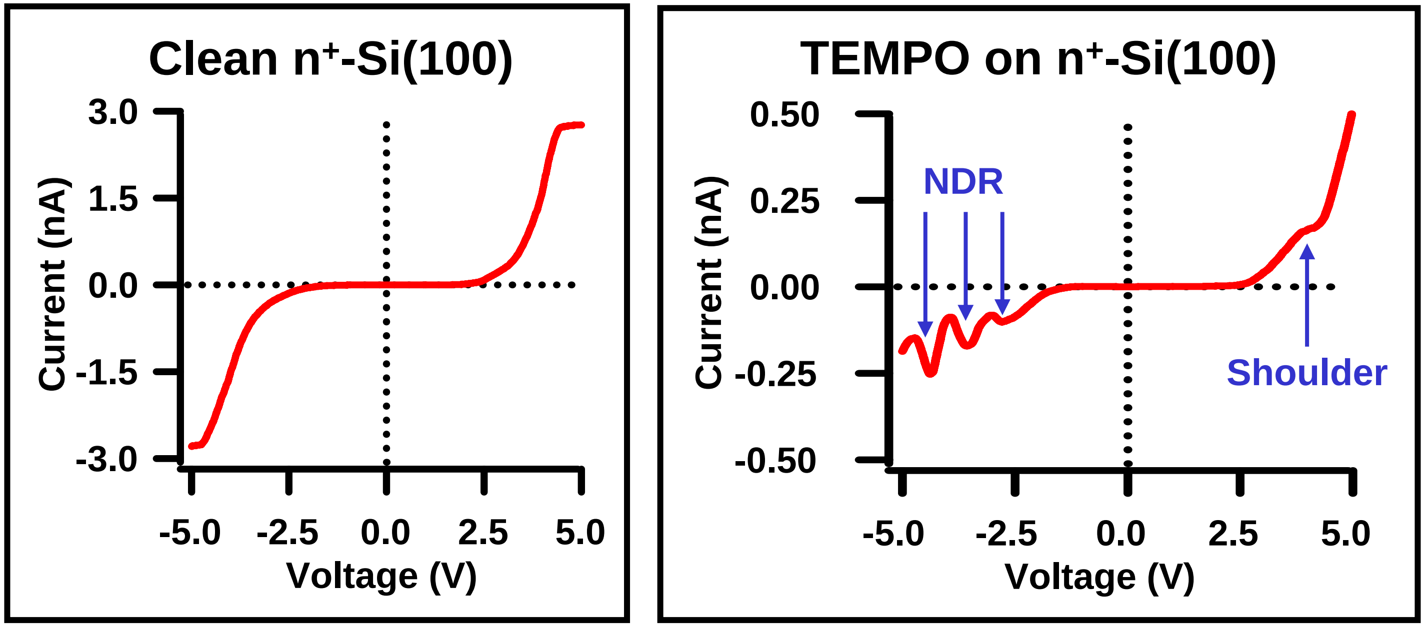

- Multiple NDR events.
- NDR is only observed at negative sample bias.
- Shoulder is only observed at positive sample bias.

Band Diagrams for Molecules on n$^+$-Si(100)

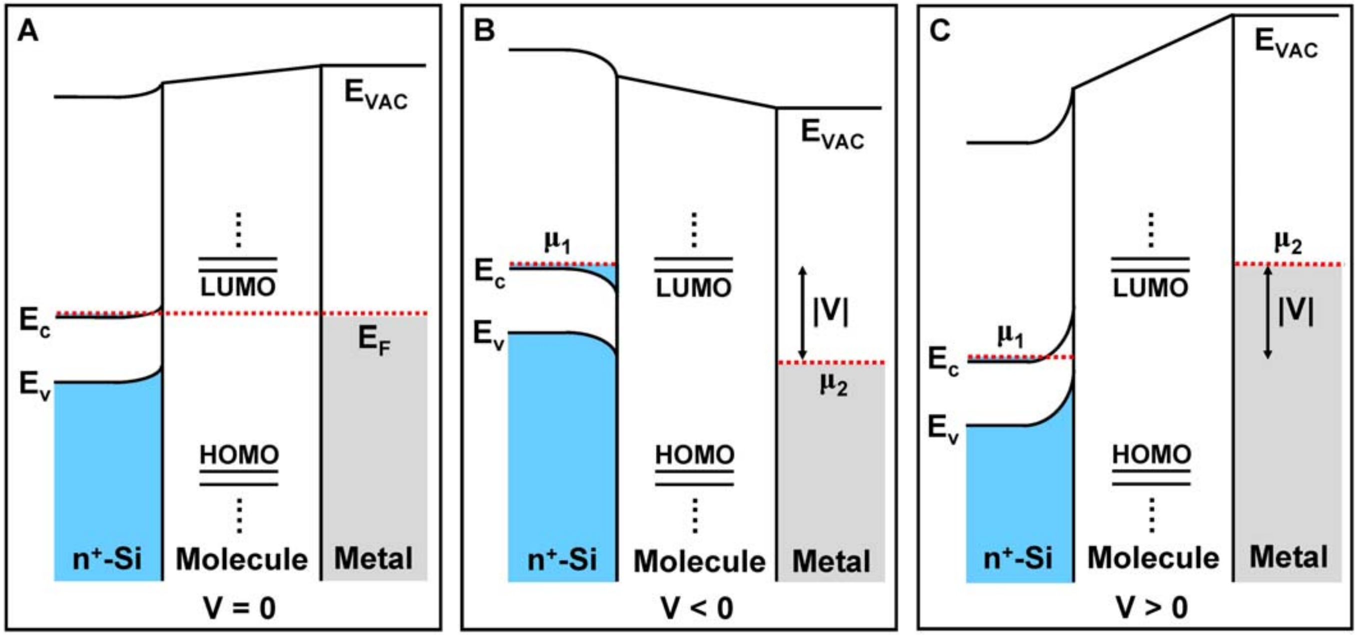

Equilibrium **NDR** **Shoulder**

For p$^+$-Si(100), the behavior should be qualitatively the same, except at the opposite bias polarity.

NDR for TEMPO on p$^+$-Si(100)

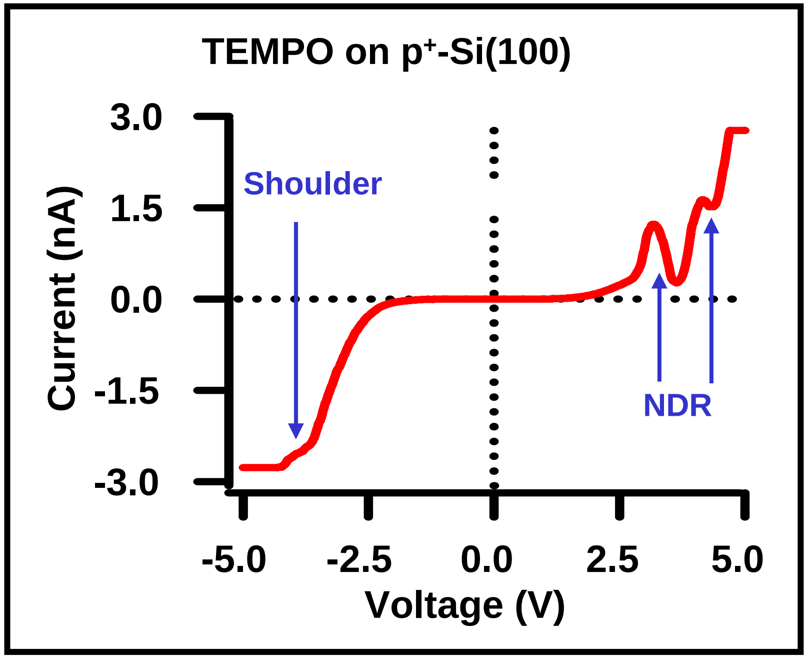

- Qualitatively similar behavior to TEMPO on n$^+$-Si(100) except opposite polarity, as expected.

Molecular Electronics

To become commercially viable, many obstacles must be overcome:

(1) Macroscopic contacts, interconnections

(2) Integration with conventional devices

(3) Reliability

(4) Reproducibility

→ Defect tolerant architectures and nanotube electronics help circumvent some of these problems

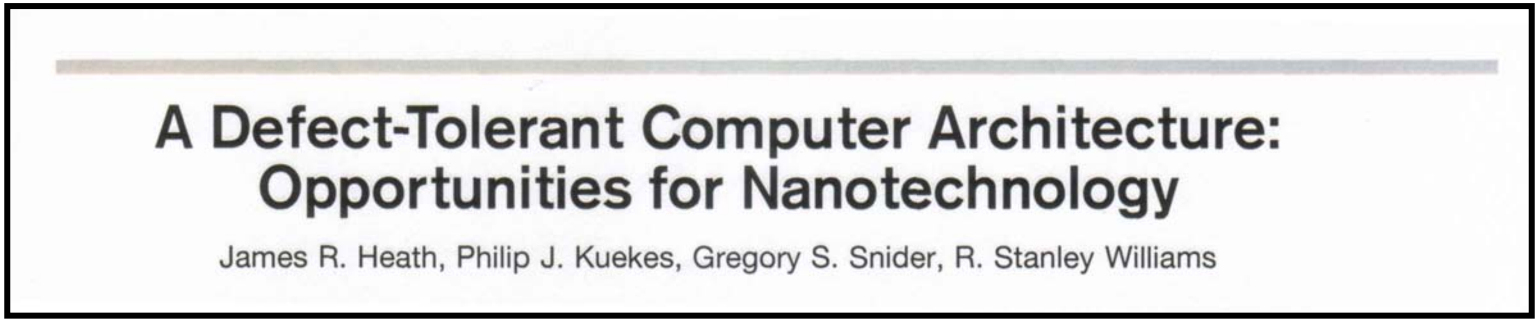

A Defect-Tolerant Computer Architecture: Opportunities for Nanotechnology

James R. Heath, Philip J. Kuekes, Gregory S. Snider, R. Stanley Williams

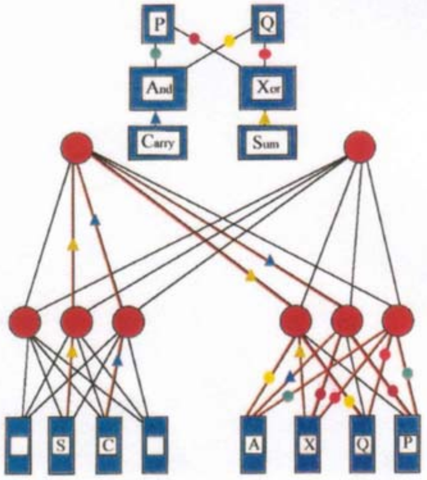

Fig. 3. This figure demonstrates how a particular implementation of a custom configurable computer is downloaded onto a given set of resources, and how the crossbar architecture, with sufficient bandwidth, allows for defect-tolerant computation. The blue boxes at the bottom are logic elements or memory (or both). The role of this system is to add two bits, P and Q, together to produce a Sum (S) and a Carry (C). When P and Q are the inputs to an And gate (A), then the output is the Carry. When they are inputs into an Xor gate, then the output is the Sum. Thus, both P and Q must be connected to both A and X, and the ouput of A and X must be connected to the memory locations for S and C, respectively. The red circles are crossbars, and there are two levels to this fat tree. This particular logical implementation illustrates how various components with widely varying numbers of defect can still be used to construct a working system. From the bottom left crossbar, and proceeding clockwise, we use 20, 70, 0, and 80% of the available resources. Similar arguments can be made for the other components. To understand this system more completely, it is advisable to reassign the look-up tables differently, define some of the crossbar switches to be defective and thus removed from the available resources, and then reconnect the system to enable the adder. Such an exercise is very similar to what the compiler does when it downloads the logical architecture onto the available resources.

J. R. Heath, *et al.*, *Science*, **280**, 1716 (1998).